ISSN 1392-1207. MECHANIKA. Vol. 29, No. 2, 2023: 110–114

The Modified Residual Property Model for Fracture Mechanics

Goksel SARACOGLU
Faculty of Aeronautics and Astronautics, Iskenderun Technical University, 31200 Iskenderun, Hatay, Turkey,
E-mail: goksel.saracoglu@iste.edu.tr

https://doi.org/10.5755/j02.mech.31339

1. Introduction

Laminated polymeric composite materials are the preferred material group in many industries due to their high strength, fracture toughness, light weight and corrosion properties under certain conditions [1-2]. As with isotropic materials, these materials also need shape connection for assembly. Therefore, they contain geometric discontinuities in circular, elliptical and various other shapes [3-7]. These discontinuities show notch effect under stress and cause stress concentration [8].

In order for composite materials to be used safely, the stress values and crack propagation at and near the notch and crack tip must be analysed. In this context, analytical methods specific to anisotropic materials, finite element analysis method, semi-analytical methods using both analytical and finite element analysis methods have been proposed [9]. In addition, considering that each composite characteristic will require the application of micro-mechanical models, methods are also used to determine the strength stress in notched specimens by using the micro-mechanical models [10]. The 3D finite element model of composite laminates for progressive damage analysis based on continuum damage mechanics was developed [11-13].

Although laminated composite materials present a different mechanical response (fibre rupture, fibre-debonding, etc.) at and near the notch tip than isotropic materials, the methods are also used to adapt Linear Elastic Fracture Mechanics (LEFM) to composite materials on a macroscopic scale [14]. The Theory of Critical Distance (TCD) is the origin of some of these methods [15-17]. The Point Method (PM), which is the most widely used in the theory, states that fracture will occur if the stress value encountered in the load direction at a certain distance from the notch tip is equal to the tensile strength of the brittle material.

In these methods, which are generally categorised under the titles of stress and energy methods, hybrid methods have been developed in which a stress and an energy method are used together. Finite Fracture Model is one of the most frequently used methods in order to respond to the situations where the crack is very small and very large in length, and also in hybrid systems that indicate that the fracture mechanism works together with stress and energy [18]. Essentially, this method, which is another expression of LEFM in which the mathematical integrations required to express the fracture energy are performed in finite steps, contains one of the possible explanations for the ability of TCD to predict fracture conditions in notched structures. However, in terms of practicality, it is not widely used in industrial applications [19].

The loss of properties of materials over time follows a certain mathematical path, independent of the influencing factor (corrosion, impact, fatigue, notch, etc.) and material. This mathematical way is in the form of a decreasing exponential function.

The Residual Property Model (RPM) is a macro-scale method based on this differential equation. The model can give valid results up to a limit where linearity is no longer valid. To apply the model, two experimental points are needed to predict the exact variation of mechanical properties of polymeric materials as a function of energy involved, regardless of the extent of the damage and/or the source of the damage [20].

However, many of the methods described above, have two limitations: Firstly, it is analytically complicated and secondly, it requires the knowledge of at least two characteristic values of the material (such as tensile strength, characteristic distance or critical fracture values by performing at least two tests).

This study focuses on the determination of the critical fracture stresses of brittle material at various notch length ratios, albeit on a macro-scale, with one characteristic value determined by using LEFM.

2. The residual property method

The Residual Property Model (RPM) is used to describe the residual mechanical properties of materials after damage. The model gives results close to actual values for changes in material properties, regardless of the cause of the damage and the type of material handled. The model is based on an exponential decay law of the mechanical degradation of a material due to damage as in Eq. (1) [20]:

$$\frac{P_r}{P_0} = 1 - e^{-u}, \tag{1}$$

where: P_r is the residual property value related for the notch length currently considered; P_0 is the original value of the same property for the un-notched sample (for example, the material tensile strength), and u is a function of each notch length a and sample width W.

According to the model, the deterioration of a feature due to notch is explained by the Eq. (2):

$$s = y + \frac{1}{s}\frac{dy}{dM}, \tag{2}$$

where: $y = \frac{P_r}{P_0}; M = \frac{a}{W}; s = \frac{P_\infty}{P_0}$.

Considering a cracked material M is the ratio of crack length to sample width. The closer the a/W ratio is to 1, the closer the dy/dM will be to 0, indicating that the material has no significant mechanical properties. In this case, P_r/P_0 will converge to s. Solving the differential equation of the RPM model, Eq. (3) is reached:

$$\frac{P_r}{P_0} = s + (1-s)^{-sM}. \quad (3)$$

In this case, as M (representing a/W) approaches 0, P_r/P_0 will approach 1.

The feature that makes this model equal with other models is that it needs two tests to determine P_∞ and P_0 values. In the method proposed below, the critical fracture stresses given by the method are obtained with only one data.

3. The proposed method

In the proposed method, Eq. (1) is simplified as seen in Eq. (4). When u, the length function of the notch, takes its maximum value of 5, the value of e^{-u} reaches about 0.67. This indicates that the load-carrying strength of the material is almost gone compared to the initial state without notch.

A material releases energy following a nonlinear curve, as shown in Fig. 1. The abscissa of the graph shows the exponent u of the function e^{-u}, and the ordinate shows the ratio of the fracture stress σ_r to the tensile strength σ_0 as seen in Eq. (4):

$$e^{-u} = \frac{\sigma_r}{\sigma_0}. \quad (4)$$

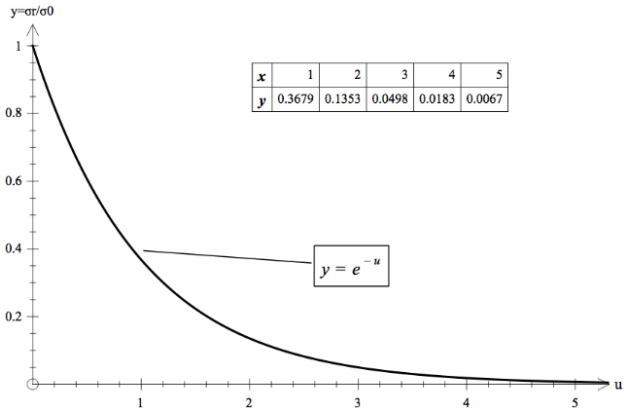

Fig. 1 The descending exponential curve giving the σ_r/σ_0

Fig.1 shows the approximate percentage of the material's residual energy at each integer value of u based on increasing crack length. This type of curve follows a precise mathematical formula and is called a descendent exponential curve. The released strain energy curve is a decreasing exponential.

In Fig. 2, there is a hyperbolic notch in a part subjected to stress in both directions. The tip radius of curvature of the notch is ρ. The coordinate system starts inside the notch-tip by $r = \rho/2$. When ρ / a (a, half the crack length) is small compared to one, the origin is very close to the focal point of the ellipse or hyperbola representing the surface of the crack. This field equation in the load direction is similar to that for a "mathematically sharp" plane crack [21].

The elastic stress distribution in the load direction adjacent to the elliptical holes and hyperbolic notches will be as in Eq. (5) [21]. K_I and σ_y represents the Mode-I stress intensity factor and the stress in the load direction near the notch tip, respectively:

$$\sigma_y = \frac{K_I}{(2\pi r)^{1/2}} \cos\frac{\theta}{2}\left[1 + \sin\frac{\theta}{2}\cos\frac{3\theta}{2}\right] + \frac{K_I}{(2\pi r)^{1/2}} \frac{\rho}{2r}\cos\frac{3\theta}{2}. \quad (5)$$

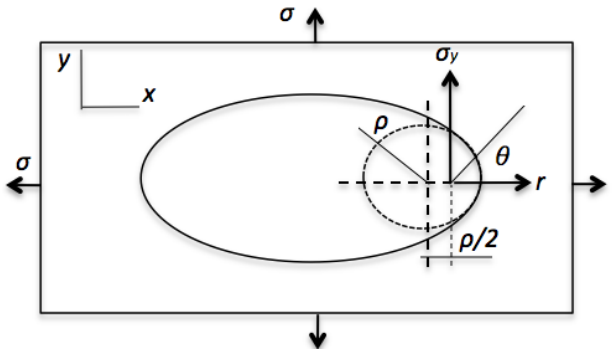

Fig. 2 Stress field coordinate system at hyperbolic notch tip [21]

$\theta = 0°$ and $r = \rho/2$ should be used for the maximum stress in the load direction at the crack tip as seen in Eq. (6):

$$\sigma_{max} = 2K_I / (\pi\rho)^{1/2}. \quad (6)$$

Whether the tip radius of the defect is small or large, fracture will occur when the stress intensity factor K_I at the tip reaches the fracture toughness of the material. Therefore, by giving a value of 1.2732 mm to the ρ, the value of the stress intensity factor in σ_y is determined.

In order to determine the stress σ_y at the tip, it is necessary to start the ordinate and abscissa of $\sigma_y - r$ from the tip of the flaw (Fig. 3). The stress distribution in front of the flaw tip is determined by Eq. (7):

$$\sigma_0 = \frac{K_I}{(2\pi r)^{1/2}} = \frac{\sigma_y}{(2\pi r)^{1/2}}. \quad (7)$$

When the value of K_I in Eq. (7) is stated as σ_y, the tensile strength σ_0 will occur at a distance of r from the notch tip. Since the equivalent of $2\pi r$ is $\pi\rho$, the expression of the stress intensity factor depending on the tensile strength and ρ is obtained as seen in Eq. (8).

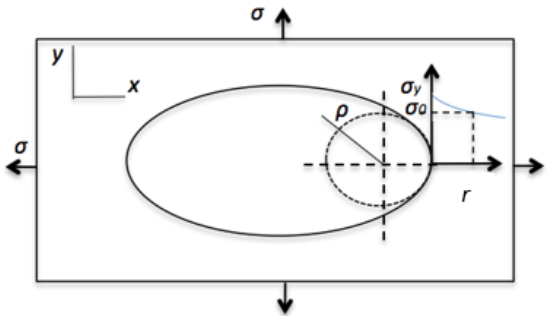

Fig. 3 Stress field coordinate system in front of the hyperbolic notch tip

$$K_I = \sigma_0 (\pi\rho)^{1/2} \quad (\rho = 1.2732\text{mm}). \quad (8)$$

In LEFM, stress intensity factor is stated by Eq. (9). The geometric correction factors Y for various test specimens are given in [22].

$$K_I = \sigma_r Y (\pi a)^{1/2}. \quad (9)$$

Regardless of the crack size, Eq. (8) and (9) will give the same result for material toughness. When Eq. (8) and (9) are set equal to each other and the ratio σ_r/σ_0 is denoted by e^{-u}, the equivalent of the exponential u is found. Thus, the exponent u will depend on the crack length a and the geometric correction factor Y as seen in Eq. (10):

$$u = lnY - \frac{1}{2} ln\left[\frac{\rho}{a}\right] (\rho = 1.2732\text{mm}). \quad (10)$$

Eqs. (4) and (10) will yield all the critical fracture stresses including approximate tensile strength with only single fracture test data of any kind of specimen. For the clamped-end single-edge cracked tensile and compact-tension specimens, the geometric factor given in [22] should be used as seen in Eq. (11):

$$u = -\frac{1}{2} ln\left[\frac{\rho}{Ya}\right] (\rho = 1.2732\text{mm}). \quad (11)$$

The σ_0 or the σ_r for all crack lengths can be approximately determined using Eqs. (4) and (10) or (11) depending on specimen loading condition.

The same approach can be applied to circular holes. The maximum stress that will occur at the edge of a hole of radius R in the specimen under the tensile stress will have the equality as seen in Eq. (12):

$$\sigma_y = \frac{2K_I}{(\pi R)^{1/2}} = K_t \sigma_r. \quad (12)$$

The σ_y is also denoted as the critical fracture stress σ_r multiplied by the stress concentration factor K_t on the right-hand side of the Eq. (12).

The stress concentration factor for a very small length of crack propagating from the edge of the hole will be as in Eq. (13) [23]:

$$K_t = 1 + 2\left[\frac{\rho}{a}\right]^{1/2}. \quad (13)$$

Since the theoretical ρ of 1.2732 mm is the equivalent of $4/\pi$, Eq. (12) and (13) can be linked. As a result of this connection, Eq. (14) is reached:

$$K_t = 1 + \frac{4}{(\pi R)^{1/2}}. \quad (14)$$

If the stress concentration K_t is taken as in Eq. (14) and the stress intensity K_I is taken as in Eq. (8) and put in Eq. (12), σ_r/σ_0 is obtained as in Eq. (15):

$$\frac{\sigma_r}{\sigma_0} = \left[\frac{2(\pi\rho)^{1/2}}{4 + (\pi R)^{1/2}}\right] \frac{1}{Y^2} (\rho = 1.2732\text{mm}). \quad (15)$$

The factor Y in Eq. (15) is included to consider the effect of the specimen edge on the hole edge. The Y is the polynomial equation of the central crack specimen [22].

The exponent u is found for the circular hole as seen in Eq. (16). The ρ in the equation is equal to 1.2732 mm:

$$u = ln\left[4 + (\pi R)^{1/2}\right] + 2lnY - ln\left[2(\pi\rho)^{1/2}\right]. \quad (16)$$

The σ_0 or σ_r for all circular hole defects can be approximately determined using Eqs. (4), (15) and (16).

4. The model verification

The proposed approach has been applied to $[0/90/\pm45]_{ns}$ Thornel T300 carbon fiber/epoxy laminated composite including crack (three-point bending-TPB) and central circular hole tensile specimen (Fig. 4). The results of them were examined in their studies [24-25]. The σ_0, E_{11}, E_{22}, and υ_{12} are 581 MPa, 138 GPa, 11 GPa and 0.35, respectively. The proposed method was compared with the experimental results.

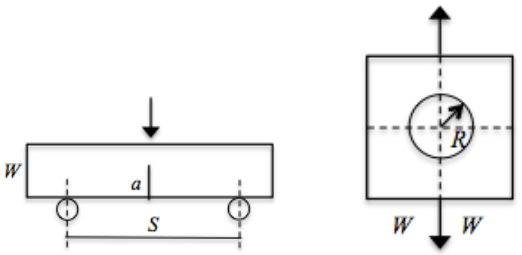

a b

Fig. 4 $[0/90/\pm45]_{ns}$ spec: a) TPB: b) circ. hole schem. view

The first sample is the three-point bending (TPB) specimen (Fig. 4, a) [24]. Table 1 is based on the tensile strength for the proposed method. When the results are analysed in Table 1 according to actual ones, it is seen that the method has a deviation rate between +3.84% and –3.47% range. The related graphical representation is given in Fig. 5.

Table 1

TPB test results comparison (in MPa)

a/W	Exp.	DZM	IFM c_0=1.64 mm	PSC d_0=0.63 mm	Eq. (10) and (4)
0.24	269	269 (Ref.)			267
0.36	202	198	205	195	196
0.48	144	140	149	139	139
0.60	92	92	100	92	92
0.72	52	54	62	56	54

In the 140×316 mm^2·($2W$ = 140 mm) specimen with a hole with a radius of 5 mm (Fig. 4, b), the radius of the hole was kept constant and the width of the specimen was changed, as can be seen in the first column of Table 2, in its study [25].

When the proposed method is used, critical fracture stresses were determined with an error margin of +4.6% to –2.9%. The DZM has a deviation range of +1.4% to –5.3%, and the IFM has the range of +6% to –11.2% as seen in Table 2. The graphical representation is given in Fig. 6.

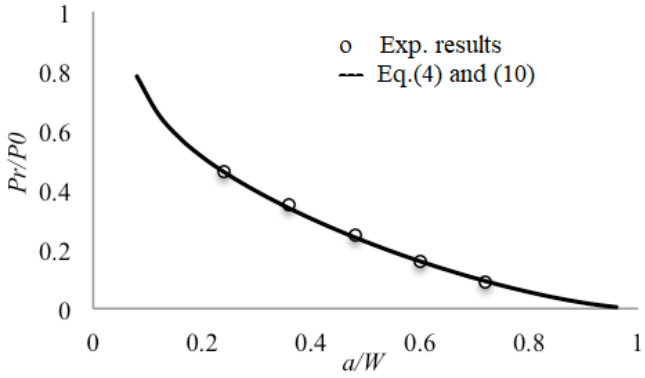

Fig. 5 The comparison of actual and predicted rates of TPB specimen

Table 2

Predicted critical stresses (R = 5 mm circular holes of various ratios W/W_0 (in MPa)

W/W_0	Exp.	DZM	IFM c_0=1.64 mm	Eq. (16) and (4)
1.	284	288	301	291
2/3	290	286	294	290
1/2	285	282	286	288
1/3	276	268	263	284
1/4	267	253	247	264
1/5	237	236	229	248
1/7	206	195	183	207

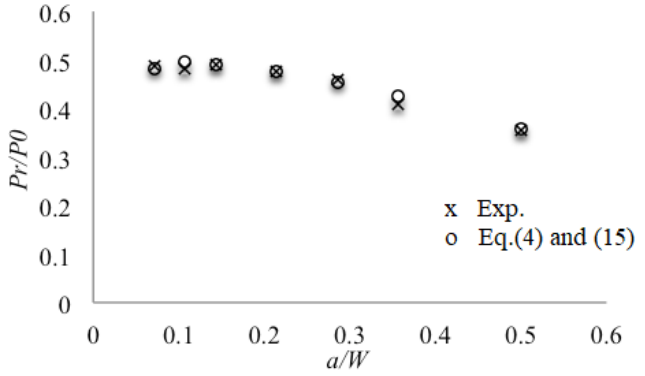

Fig. 6 The comparison of actual and predicted rates with R = 5 mm hole at various R/W ratios

5. Conclusions

In this study, the critical fracture stress values of a material containing a crack or a hole were obtained by using a stress field function based on a coordinate system starting from $r = \rho/2$ inside the defect in a specimen containing an elliptical defect. The stress intensity factor is equal in value to the stress value at the defect tip, which will facilitate the calculations. Accordingly, this equality was achieved by taking the tip radius of the defect as 1.2732 mm. The main idea here is that the fracture toughness value is independent of the geometry of the defect or the part. When the stress intensity factor at the flaw tip reaches the fracture toughness, fracture will occur. Note that Eq.6 is similar to the asymptotic critical distance equation in the Finite Fracture Method [18] as seen Eq. (17):

$$\Delta s = \frac{2}{\pi}\left[\frac{K_{IC}}{\sigma_u}\right]^2. \quad (17)$$

Although similar equations have been reached from different perspectives, this study is different in that other data can be determined with only one datum, independent of the size of the defect. Another advantage is that it is a simple approach.

The Residual Property Model is an important approach to finding intermediate values by reducing the variety of factors affecting the material to a differential equation. However, with this study, it will be possible to determine these values with only one datum in terms of Fracture Mechanics.

References

1. **Warren, K. C.; Lopez-Anido, R. A.; Vel, S. S., Bayraktar, H. H.** 2016. Progressive failure analysis of three-dimensional woven carbon composites in single-bolt, double-shear bearing, Composites B 84: 266–276. https://doi.org/10.1016/J.COMPOSITESB.2015.08.082.
2. **Isart, N.; Said, B. El., Ivanov, D. S.; Hallett, S. R.; Mayugo, J. A.; Blanco, N.** 2015. Internal geometric modelling of 3D woven composites: A comparison between different approaches, Compos. Struct. 132: 1219-1230. https://doi.org/10.1016/J.COMPSTRUCT.2015.07.007.
3. **Caminero, M. A.; Lopez-Pedrosa, M.; Pinna, C.; Soutis, C.** 2013. Damage monitoring and analysis of composite laminates with an open hole and adhesively bonded repairs using digital image correlation, Composites B 53: 76-91. https://doi.org/10.1016/J.COMPOSITESB.2013.04.050.
4. **Ceritbinmez, F.; Yapici, A.; Kanca, E.** 2021. The effect of nanoparticle additive on surface milling in glass fiber reinforced composite structures. Polymers and Polymer Composites, 29, S575 - S585. https://doi.org/10.1177/09673911211014172.
5. **Khashaba, U. A.** 2012. Drilling of polymer matrix composites: A review, J. Compos. Mater. 47: 1817-1832. https://doi.org/10.1177/0021998312451609.
6. **Bao, H.; Liu, G.** 2016. Progressive failure analysis on scaled open-hole tensile composite laminates, Compos. Struct. 150: 173-180. https://doi.org/10.1016/J.COMPSTRUCT.2016.05.017.
7. **Khashaba, U. A.; Khdair, A. I.** 2017. Open hole compressive elastic and strength analysis of CFRE composites for aerospace applications, Aerosp. Sci. Technol. 60: 96-107. https://doi.org/10.1016/J.AST.2016.10.026.
8. **Anitha Priyadharshani, S; Meher Prasad, A.; Sundaravadivelu, R.** 2017. Analysis of GFRP stiffened composite plates with rectangular cutout, Compos. Struct. 169: 42-51. https://doi.org/10.1016/J.COMPSTRUCT.2016.10.054.
9. **Sevenois, R.; Koussios, S.** 2014. Analytic methods for stress analysis of two-dimensional flat anisotropic plates with notches: An overview, ApMRv 66: 060802. https://doi.org/10.1115/1.4027562.
10. **Vignoli, L. L.; Savi, M. A.; Pacheco, P. M. C. L.; Kalamkarov, A. L.** 2020. Multiscale approach to predict strength of notched composite plates, Compos. Struct. 253: 112827. https://doi.org/10.1016/j.compstruct.2020.112827.

11. **Han, W.; Hu, K.; Shi, Q.; Zhu, F.** 2020. Damage evolution analysis of open-hole tensile laminated composites using a progress damage model verified by AE and DIC, Compos. Struct. 247: 112452. https://doi.org/10.1016/j.compstruct.2020.112452.
12. **Divse, V.; Marla, D.; Joshi, S. S.** 2021. Finite element analysis of tensile notched strength of composite laminates, Compos. Struct. 255: 112880. https://doi.org/10.1016/j.compstruct.2020.112880.
13. **Guo, Q.; Zhang, Y.; Li, D.; Li, M.; Sun, X.; Chen, L. M.** 2021. Tensile properties and failure mechanism of 3D woven composites containing holes of different geometries, Thin-walled Structures 166: 108115. https://doi.org/10.1016/J.TWS.2021.108115.
14. **Awerbuch, J.; Madhukar, M. S.** 1985. Notched strength of composite laminates: predictions and experiments-a review, Journal of Reinforced Plastics and Composites. https://doi.org/10.1177/073168448500400102.
15. **Taylor, D.** 2007. The theory of critical distances: a new perspective in fracture mechanics. New York: Elsevier.
16. **Susmel, L.** 2008. The theory of critical distances: a review of its applications in fatigue, Eng. Fract. Mech. 75: 1706–1724. https://doi.org/10.1016/J.ENGFRAC-MECH.2006.12.004.
17. **Taylor, D.** 2008. The theory of critical distances, Eng. Fract. Mech. 75: 1696–1705. https://doi.org/10.1016/b978-0-08-044478-9.x5000-5.
18. **Cornetti, P.; Pugno, N. M.; Carpinteri, A.; Taylor, D.** 2006. Finite fracture mechanics: A coupled stress and energy failure criterion, Engineering Fracture Mechanics 73: 2021-2033. https://doi.org/10.1016/J.ENGFRAC-MECH.2006.03.010.
19. **Delprete, C.; Maggio, L.; Sesana, R.** 2021. Theory of critical distances: a discussion on concepts and applications, Proceedings of the Institution of Mechanical Engineers, Part C: Journal of Mechanical Engineering Science 235: 5695-5708. https://doi.org/10.1177/0954406220985887.
20. **Papanicolaou, G. C.; Samoilis, G.; Giannis, S.; Barkoula, N. M.; Karger-Kocsis, J.** 2002. A Model for the Accurate Prediction of the Residual Strength after Damage Due to Impact and Erosion of FRPs. https://doi.org/10.1007/0-306-48410-2_17.
21. **Creager, M.; Paris, P.** 1967. Elastic field equations for blunt cracks with reference to stress corrosion cracking. International Journal of Fracture Mechanics, Volume 3, pp. 247-252. https://doi.org/10.1007/BF00182890.
22. **Tada, H.; Paris, P. C.; Irwin, G. R.** 2000. The Stress Analysis of Cracks Handbook, Third Edition. ASME Press, New York. https://doi.org/10.1115/1.801535.
23. **Pilkey, W. D.; Pilkey, D. F.** 2008. Peterson's stress concentration factors. Third edition. John Wiley & Sons, Inc., Hoboken, New Jersey. https://doi.org/10.1002/9780470211106.
24. **Aronsson, C.; Backlund, J. C.** 1986. Tensile fracture of laminates with cracks, Journal of Composite Materials 20: 287 - 307. https://doi.org/10.1177/002199838602000305.
25. **Backlund, J. C.; Aronsson, C.** 1986. Tensile fracture of laminates with holes, Journal of Composite Materials 20: 259 - 286. https://doi.org/10.1177%2F002199838602000304.

G. Saracoglu

THE MODIFIED RESIDUAL PROPERTY MODEL FOR FRACTURE MECHANICS

S u m m a r y

In this paper, the application requirement of the Residual Property Model based on the decrescent exponential function is reduced to only one mechanical test datum. For this, by using Creager and Paris's elastic stress field equation in front of the blunt elliptical hole, the theoretical radius was chosen for the tip curvative and the maximum stress in the load direction at the tip is ensured to be equal the fracture toughness. Thus, the workload of the model is reduced by making the u exponent in the e^{-u} function dependent on the geometric correction factor and the crack length. It was applied to the laminated composite specimens with three-point bending and the specimens including circular hole, and critical fracture stress values close to actual values were achieved.

Keywords: fracture toughness, fracture stress prediction, stress concentration factor, stress intensity factor, the residual property model.

Received May 9, 2022
Accepted April 5, 2023